Dual-stimuli responsive single-chain polymer folding via intrachain complexation of tetramethoxyazobenzene and beta-cyclodextrin

Daniel C. Lee,[1] Kathryn N. Guye,[2] Rajan K. Paranji,[2] Kacper Lachowski,[3] Lilo D. Pozzo,[3] David S. Ginger, [2] Suzie H. Pun[1,4*]

[1]Molecular Engineering & Sciences Institute, [2]Department of Chemistry, [3]Department of Chemical Engineering, [3]Department of Bioengineering

University of Washington, Seattle, Washington 98195, United States

ABSTRACT: We synthesize and characterize a tri-block polymer with asymmetric tetramethoxyazobenzene (TMAB) and β-cyclodextrin functionalization, taking advantage of the well-characterized azobenzene derivative-cyclodextrin inclusion complex to promote photo-responsive, self-contained folding of the polymer in an aqueous system. We use ^{1}H NMR to show the reversibility of (E)-to-(Z) and (Z)-to-(E) TMAB photoisomerization, and evaluate the thermal stability of (Z)-TMAB and the comparatively rapid acid-catalyzed thermal (Z)-to-(E) isomerization. Important for its potential use as a functional material, we show the photoisomerization cyclability of the polymeric TMAB chromophore and calculate isomerization quantum yields by extinction spectroscopy. To verify self-inclusion of the polymeric TMAB and cyclodextrin, we use 2-D ^{1}H NOESY NMR data to show proximity of TMAB and cyclodextrin in the (E)-state only; however, (Z)-TMAB is not locally correlated with cyclodextrin. Finally, the observed decrease in photoisomerization quantum yield for the dual-functionalized polymer compared to the isolated chromophore in an aqueous solution confirms TMAB and β-cyclodextrin not only are in proximity to one another, but also form the inclusion complex.

Molecular switches, motifs that undergo chemical changes in response to external stimuli, have been incorporated into nanoparticle and polymer systems to achieve functional materials. By controlling molecular motion on the nanoscale, researchers have been able to design materials for applications such as nanoactuation,[1–3] drug delivery,[4–6] catalysis,[7,8] and sensing.[7,9]

We were particularly interested in developing a synthetic polymer system that exhibits photoresponsive folding behavior in solution. Light is an attractive stimulus as it can be (1) applied noninvasively from a distance, (2) temporally and spatially controlled, and (3) different wavelengths can be used to selectively activate different chromophores.

Folding behavior has been explored in both biopolymer and synthetic systems, and can be observed by changes in fluorescence between Förster resonance energy transfer pairs,[10] resonant frequencies between plasmonic dimers,[11,12] and electron spin resonance spectra between nitroxide spin labels.[13] More macroscopic changes in the biopolymer have been measured without labeling via circular dichroism[14] and nuclear Overhauser effect (NOE) nuclear magnetic resonance (NMR) experiments.[15]

In synthetic polymer systems, folding behavior can be achieved by placing bonding or complexing molecular pairs at different positions along the polymer main chain. For example, folding polymers of different architectures have been achieved by placing alkynes in different positions along the polymer main chain and covalently stapling them with azide-alkyne click chemistry.[16] In contrast, reversibly folding polymers can be realized by placing stimuli-responsive molecular pairs on the α- and ω- ends of a polymer. One of the earliest reports of reversible folding behavior involved the use of a short oligo(ethylene glycol) chain with anthracenes on the α- and ω- ends that can photodimerise to lock the folded chain.[17] Such α-/ω-complexation has been further explored to make reversibly folding polymers using hydrogen donor-acceptor pairs,[18,19] metal-ligand complexes,[20] host-guest pairs including β-cyclodextrin (βCD).[21,22]

We set out to further develop these concepts further with a folding polymer that was of high molecular weight and could reversibly fold in response to multiple stimuli. Because large polymers in water often exhibit complicated solution phase behavior as a function of temperature, we wanted to avoid heat as one of the stimuli. Of the many molecular recognition pairs in the literature, the azobenzene-cyclodextrin pair offers attractive features of photoreversible complexation, relative ease of synthesis and derivatization, and subsequent tunable properties.[23–25] Azobenzenes have gained significant attention due to their ability to undergo reversible (E)-to-(Z) isomerization in response to temperature[26] and different wavelengths of light,[23] and have even been used to control polymer morphology[27–29] and solution self-assembly.[30–33] (E)-Azobenzenes complex with cyclodextrin in water to reduce the entropic penalty of water ordering around the hydrophobic (E)-azobenzenes and the hydrophobic inner core of cyclodextrin. (Z)-azobenzenes, however, often exhibit much lower equilibrium association constant (K_a) with cyclodextrins, due to the hydrophilic dipole perpendicular to the azo bond and the steric interference between non-planar (Z)-azobenzene and the fixed diameter of the cyclodextrin inner core. Azobenzene-cyclodextrin pairs have already been used in stimuli-responsive reversible hydrogels,[34–36] drug release,[25,37,38] material property modulation,[39,40] and supramolecular assembly.[36,41,42]

We identified tetramethoxyazobenzene (TMAB) and β-CD as our molecular recognition pair of choice. βCD shows preferential binding of (E)-TMAB (K_a = 1546 M^{-1}) over (Z)-TMAB (K_a = 82.1 M^{-1}).[25] Although the azobenzene/αCD pair exhibits ~150-fold selectivity for (E)-azobenzene (while TMAB/βCD exhibits ~20-fold selectivity), functionalization of αCD is notoriously difficult and unfunctionalized azobenzenes are not multi-stimuli responsive. The ratio of (E)/(Z)-TMAB can be modulated using multiple stimuli, including heat, light, and Brønsted acids.[43] In particular, the presence of Brønsted acids catalyzes the (Z)-to-(E) isomerization[44,45] and shifts the equilibrium to (E)-TMAB via formation of an intramolecular hydrogen bonding 6-membered species.[43]

Herein we report the synthesis and characterization of a multi-stimuli responsive high molecular weight folding polymer (**poly1**). **Poly1** is a triblock copolymer with multiple TMAB and βCD moieties and can be reversibly unfolded by photoinduced (Z)-to-(E) isomerization of TMAB. **Poly1** can also be irreversibly unfolded under acidic conditions; even though introduction of acids favors (E)-TMAB, the protonated (E)-TMAB is no longer hydrophobic and does not complex with βCD (Scheme 1). Folding behavior was characterized by illumination-dependent extinction spectroscopy and 2-D NOE NMR experiments.

Quantifying the photoisomerization behavior of TMAB in an aqueous environment. TMAB displays a characteristic double-peak extinction spectrum representing the π-π* and n-π* transitions. Unlike unmodified azobenzene which requires UV light for (E)-to-(Z) isomerization, TMAB undergoes photoisomerization with visible light in both directions. When exposed to 523 nm light, (E)-TMAB isomerizes to the less thermally stable (Z)-TMAB which can be observed as a decreasing intensity and blueshift of the π-π* extinction peak at 320 nm, as well as a blueshift of the n-π* peak at 446 nm. Rapid photoisomerization from (Z)-to-(E) can be obtained by 470 nm illumination.[46] We observe this process by red-shifting of both extinction peaks and an increased extinction intensity of the π-π* peak.

We first sought to determine if a pendent TMAB moiety on a polymer side chain would retain its photoisomerization behavior by using a small molecule model compound triethyleneglycol-functionalized TMAB (TMAB-TEG) in D_2O. First, we determined the photostability of TMAB-TEG upon exposure to ambient light. Samples were exposed to either 470 or 523 nm LED light (LED Engin) until there were no observable changes in the (E)/(Z) ratio by ^{1}H NMR spectroscopy. When further irradiation generated no additional TMAB isomerization, the sample was exposed to ambient light for up to 30 minutes and the (E)/(Z) ratio was measured again. We found that TMAB-TEG retains its photoisomerization behavior as measured by 1H NMR spectroscopy in D_2O respectively (Figure 1a). We also found that TMAB-methacrylate in DMSO-*d6* also exhibits its photoisomerization behavior (Supporting Info S1).

Second, we determined the thermal stability of (Z)-TMAB-TEG at 26.7 ºC and 45 ºC again with ^{1}H NMR spectroscopy (Figure 1b). The thermal relaxation rate in darkness was determined to be negligible over 6 hours for both 26.7 ºC and 45 ºC and all further NMR experiments were done at 25 ºC. This slow thermal relaxation enabled us to use DOSY and 2D NOESY ^{1}H NMR experiments, which take many hours, to determine polymer folding behavior.

Finally, we determined that in the presence of a small amount of deuterium chloride (DCl), the (E)-to-(Z) isomerization of TMAB is complete within 30 minutes (Figure 1c). The acid catalyzes the (Z)-to-(E) isomerization[44,45] and shifts the equilibrium to (E)-TMAB via formation of an intramolecular hydrogen bonding 6-membered species that improves its resonance stabilization.[43] Protonated TMAB exhibits higher long wavelength absorption which is consistent with its extended π-conjugation (proposed mechanism and spectrum in Supporting Info S2).

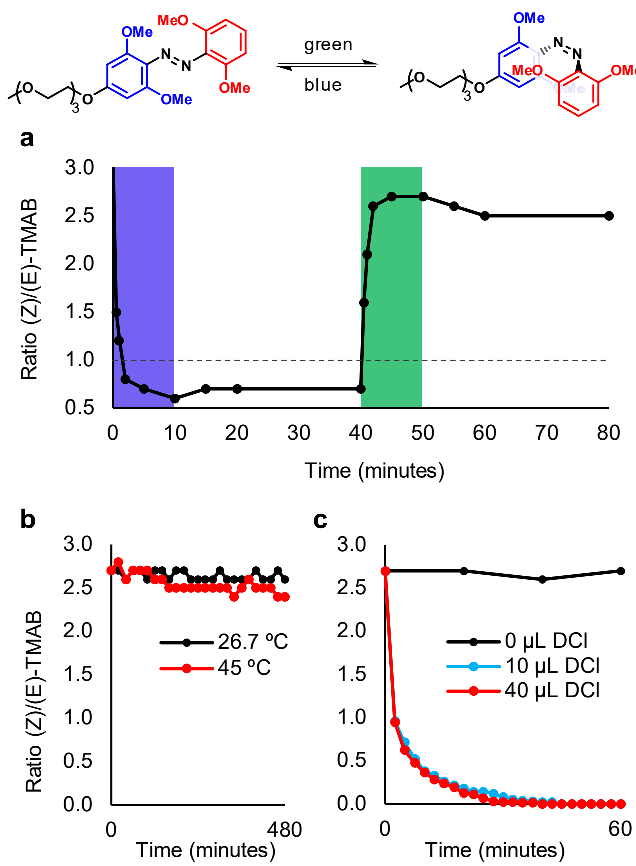

Figure 1. Quantification of TMAB-TEG (model compound) photoisomerization and relaxation by 1H NMR spectroscopic analysis. [a]Ratio of (Z) to (E)-TMAB as a function of irradiation with green or blue light. [b]Ratio of (Z) to (E)-TMAB during its thermal relaxation at 26.7 ºC or 45 ºC . [c]Ratio (Z)/(E)-TMAB during its acid catalyzed relaxation at 26.7 ºC.

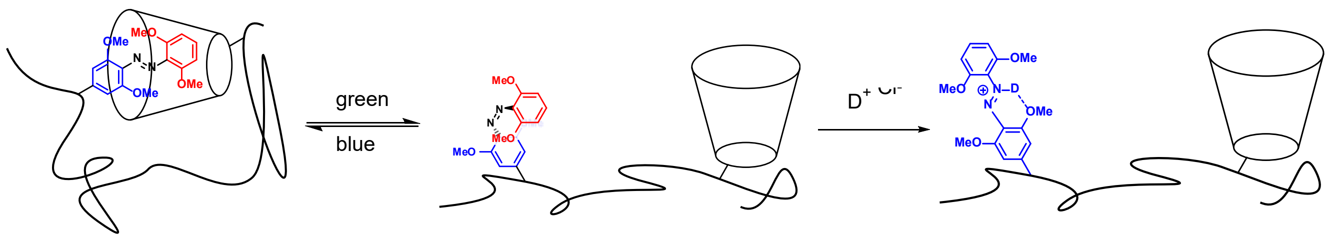

Scheme 1. Poly1 reversible photoinduced folding and unfolding and irreversible Brønsted acid induced unfolding.

Synthesis of poly1. After confirming that functionalized TMAB exhibits photoisomerization behavior, we aimed to synthesize a water-soluble polymer (poly1) with TMAB and βCD present at opposing ends of the polymer. We hypothesized poly1 would fold and unfold in response to the isomerization and protonation state of TMAB (Scheme 1). (Z)-to-(E) photoisomerization of pendent TMABs on poly1 would result in TMAB-βCD complexation and subsequent polymer folding. (E)-to-(Z) photoisomerization of pendent TMAB would result in poly1 unfolding due to the lower Ka of (Z)-TMAB and βCD. We also hypothesized that the reversible photoisomerization of TMAB and poly1 folding can be stopped via protonation of TMAB, resulting in loss of hydrophobicity and preventing subsequent βCD inclusion.

Poly1 was synthesized by sequential reversible addition-fragmentation chain-transfer (RAFT) polymerization (**Scheme 2**). To incorporate TMAB moieties into a polymer made by RAFT, TMAB-methacrylate (TMAB-MA) and βCD-methacrylate (βCD-MA) were synthesized (synthetic details in Supporting Info). The polymerization of each block was stopped at 80% conversion of monomer to polymer and then the reaction mixture was subjected to dialysis against water and was then used as a macro-CTA in the polymerization of the next block. Molecular weight data of the blocks and the final polymer were determined by gel permeation chromatography (Supporting Info S3) after irradiation green light for 30 minutes and at concentrations less than 1 mg/mL. Due to the low concentrations necessary to minimize interpolymer aggregation (as determined by DOSY ^{1}H NMR; see later section on polymer DOSY), the final polymer molecular was determined by retention time to PEG standards as opposed to light scattering. The expected molecular weight given monomer conversion and final polymer composition as determined by ^{1}H NMR spectroscopy is 60 kDa. However, the molecular weight of **poly1** using PEG retention time was determined to be 120 kDa. This discrepancy is consistent with the extended conformation of poly1. The composition of the final polymer content was determined by 1H NMR spectroscopy in DMSO-d6.

Characterization of poly1 folding. Due to the broad ^{1}H NMR signals of polymeric species, ^{1}H NMR spectroscopy could not be used to study the (E)/(Z) ratio of pendent TMABs. The photoisomerization behavior of poly1 was instead studied using the characteristic changes to the extinction spectra of TMAB upon photoisomerization, which were determined by first studying TMAB-TEG in 10% D_2O, 90% water. Alternating 523 nm and 470 nm LED illuminations revealed the photoisomerization of the TMAB chromophore in poly1 is reversible with no change in the extinction spectrum of the chromophore with repeat cycling (Figure 2a, 2b). Additionally, we determined the photoisomerization quantum yield on TMAB on poly1 and TMAB-TEG. For studies with TMAB-TEG, we used hydroxypropyl-βCD, a more water-soluble analog of βCD, to attempt to mimic the high local concentration of βCD on poly1.

When comparing the extinction spectra of poly1 to TMAB-TEG a notable 24 nm redshift of the TMAB-TEG π-π* peak is observed, which can be attributed to the formation of small micellular aggregates[47,48] in solution (Supporting Info S4). When TMAB-TEG is dissolved in excess (2-hydroxypropyl)- β-cyclodextrin (HP-βCD), the extinction spectrum is blueshifted towards the poly1 spectrum as these aggregates are disrupted by the newly formed inclusion complexes. We therefore conclude that TMAB-TEG readily includes βCD in aqueous solutions.

We next sought to confirm the occurrence of inclusion complexes between the TMAB and βCD moieties tethered to the poly1 backbone by determining the photoisomerization quantum yield of (E)-to-(Z) TMAB and comparing to the quantum yields of free TMAB-TEG and TMAB-TEG with soluble HP-βCD. Of the three solutions, folded poly1 would be expected to exhibit the lowest quantum yield for the photoinduced (E)-to-(Z) TMAB isomerization due to the high local concentration of βCD at the polymer backbone, and steric hindering of the (E)-to-(Z) isomerization of an included TMAB molecule. Isomerization of (Z)-to-(E) azobenzene is generally believed to follow a sterically unhindered inversion mechanism[49–51]. (E)-to-(Z) isomerization on the other hand, undergoes a sterically hindered rotation or hula twist, in which case the fraction of azobenzene able to undergo a (E)-to-(Z) isomerization is dependent on the local environment of the chromophore[52–54]. A more sterically crowded environment, such as on the inside of a cyclodextrin molecule, will limit the rotation of TMAB and thereby reduce the yield of (E)-to-(Z) isomerization.

We then measured the extinction spectrum of poly1 and TMAB-TEG over time (Figure 2c) at low illumination fluence, 5 mW/cm^2, with a 523 nm LED (LED Engin). Time was converted to the integrated photokinetic factor (IPF) (Supporting Info S5) to account for the absorption of 523 nm light with time while the extinction spectrum changes, effectively converting time to photon dose. Using a modified method[52] to determine the fraction of (Z)-TMAB with time, these curves were then fit to an exponential curve as

$$y_t = (y_0 - y_\infty)\exp(-Ax) + y_\infty \qquad (1)$$

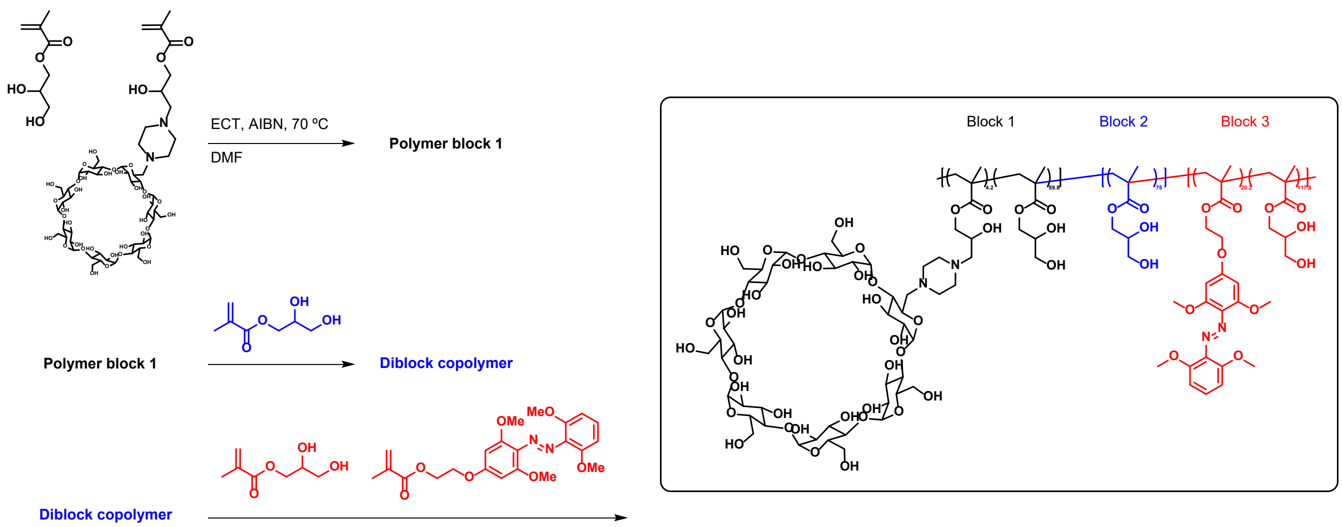

Scheme 2. Synthetic scheme for folding poly1.

where y is the fraction of (Z)-TMAB at times t, t=0, and the final photostationary state, x is the IPF, and A is the prefactor value, which is directly related to the (E)-to-(Z) quantum yield, $\Phi_{(E)}$, at 523 nm (Supporting Info S6).

From these results, we calculate a photostationary state of 83% (Z)-form for TMAB-TEG and 81% (Z)-form for poly1. For TMAB-TEG, a $\Phi_{(E)}$ of 0.34 +/- 0.01 is observed while $\Phi_{(E)}$ = 0.28 +/- 0.01 for poly1. Indeed, a decrease for $\Phi_{(E)}$ is observed for poly1, indicating inclusion of TMAB. To confirm inclusion as the source of a decreased $\Phi_{(E)}$, we repeated this experiment with the TMAB-HP-βCD solution (Figure 2c). An intermediate $\Phi_{(E)}$ of 0.32 +/- 0.01 was observed. An intermediate value is consistent with the previous extinction spectrum indicating incomplete inclusion of all TMAB chromophores in the TMAB-HP-βCD solution. We rationalize this result by taking not only solution concentration into account, but rather local concentration. As poly1 tethers TMAB and βCD within close proximity to one another, the two moieties are more likely to form an inclusion complex than untethered, individual TMAB and βCD molecules in solution.

While some studies reveal a $\Delta\Phi_{(E)}$ as large as 50% due to local steric hindrance of azobenzene isomerization, recent work by Royes et al.[55] report $\Delta\Phi_{(E)}$ of a similar magnitude for the inclusion of unmodified azobenzene with cyclodextrins in a pure aqueous solution.

We thus sought to corroborate these results with a secondary technique. We first performed small-angle neutron scattering (SANS) to determine if the radius of gyration (r_g) of poly1 changes with the isomer-state of TMAB. Folded poly1 would exhibit a lower r_g while unfolded poly1 would exhibit a higher r_g. Samples of poly1 at 1 and 5 mg/mL were prepared in D_2O and irradiated with green or blue light for 10 minutes. Unfortunately, no changes to the polymer global structure could be detected by SANS. This may be due to phase segregation or indiscriminate aggregation of poly1 in D_2O that that result in minimal changes to the global structure of poly1. These aggregates could not be disassembled by dilution in D_2O (Supporting Info S7). We attribute this behavior to be due to the poor solubility of βCD in D_2O.[56,57] Because deuterated solvents are essential for SANS, poly1 folding could no longer be analyzed by SANS.

Next, we turned to DOSY and 2-D NOESY ^1H NMR experiments to determine if poly1 exhibited photoresponsive folding behavior. 2-D NOESY NMR experiments can be used to determine if (E)-TMAB is complexed with βCD, consistent with folding. DOSY experiments can be used to determine if the TMAB-βCD NOE interactions are due to intrapolymer folding or interpolymer aggregation. We encountered two problems when we first turned to these NMR experiments. First, 2D-NOESY and DOSY NMR experiments take many hours. However, we found in our study of TMAB-TEG that the thermal relaxation of (Z)-TMAB-TEG is negligible over many hours. Second, D_2O resulted in βCD-induced aggregation. To avoid this problem in our NMR experiments, all experiments were performed in a mixture of 90% H2O and 10% D_2O. But due to the much higher intensity of the water signal in our NMR spectra, we explored two different solvent suppression pulse sequences. 3-9-19 watergate suppression did indeed suppress the water signal but also resulted in attenuation of NMR signals from the polymer. This was an important consideration because determining diffusion constants by DOSY NMR relies on signal attenuation. Instead, we used excitation sculpting zgesgp because it showed improved water suppression and no attenuation of NMR signals from the polymer. We then wrote a custom pulse program to combine excitation sculpting into DOSY experiments (Supporting info in methods).

We used our custom pulse program to determine the concentration at which poly1 was unimeric and no longer aggregating, by tracking the diffusion constant of poly1 in 90% H2O/10% D_2O. At high concentrations, interpolymer azobenzene-cyclodextrin complexation can compete with intrapolymer folding. Because interpolymer interactions are at least second order with respect to polymer concentration and intrapolymer interactions are first order with respect to polymer concentration, the polymer solution can diluted until intrapolymer folding dominates over interpolymer aggregation. The concentration at which the diffusion coefficient stops increasing with dilution is determined as the maximum concentration for the unimeric regime. Using this method, we confirmed that the single polymer concentration regime is <1.6 mg/mL by DOSY (Supporting Info S8).

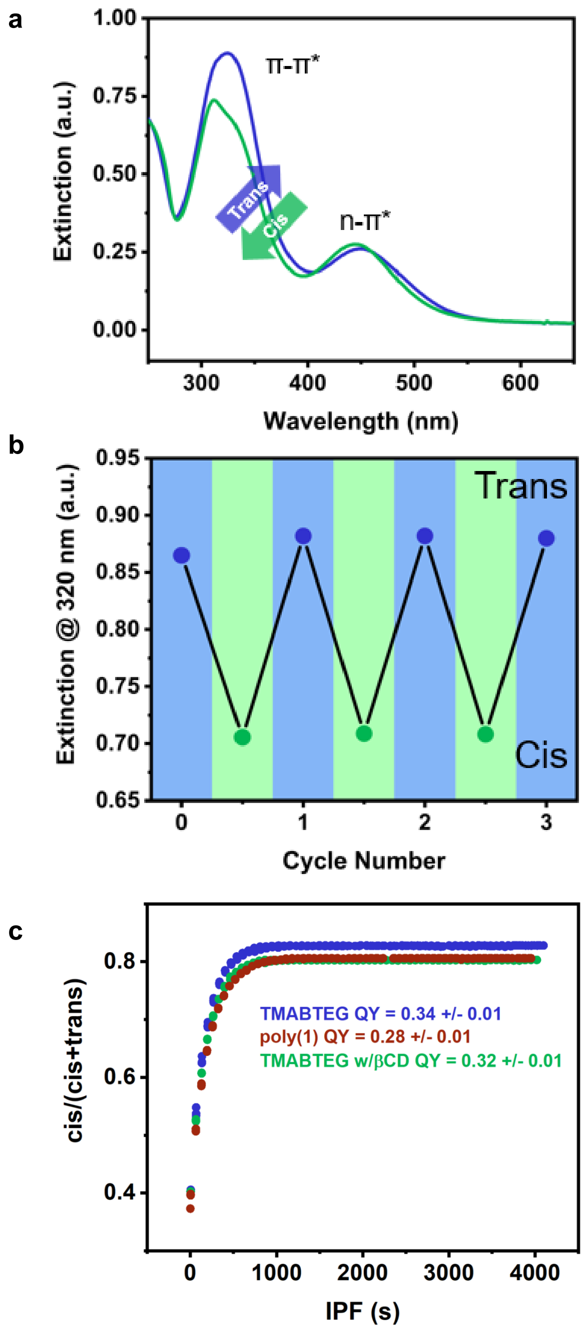

Figure 2. Quantification of TMAB photoisomerization on poly1. [a]Absorption spectrum of poly1 after irradiation with green or blue light. [b]Absorption of poly1 at 320 nm after multiple cycles of irradiation with green and blue light. [c]Determination of photoisomerization quantum yield of poly1 (red), TMAB-TEG(blue), and TMAB-HP-βCD(green).

2-D NOESY NMR with 150 μs mixing time at the single polymer concentration regime was used to determine the through-space interaction of protons on TMAB and βCD.

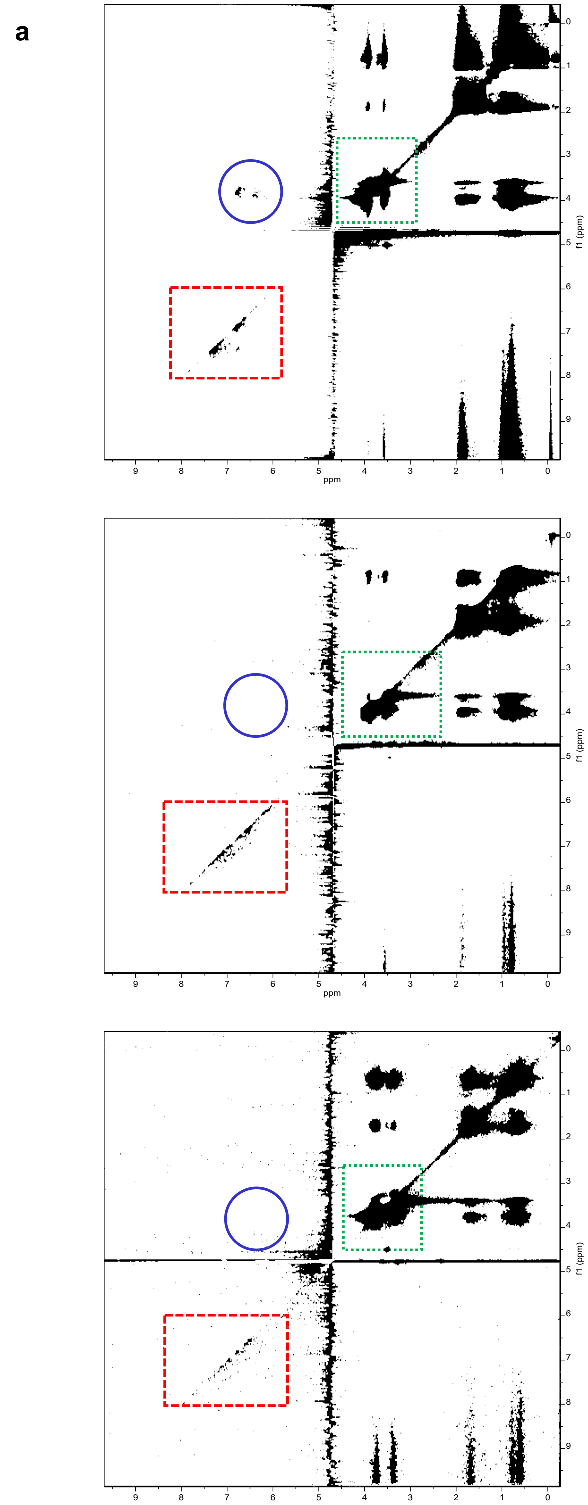

Figure 3. 2-D [1]H NOESY NMR data with cross-peaks highlighted with a blue circle. [a]Spectrum of poly1 in its folded state after irradiation with green light. [b]Spectrum of poly1 in its unfolded state after irradiation with blue light. [c]Spectrum of poly1 in its unfolded state after treatment with DCl.

2-D NOESY NMR with 150 μs mixing time at the single polymer concentration regime was used to determine the through-space interaction of protons on TMAB and βCD. TMAB/βCD cross-peaks should be observable in the folded state, and be absent in the unfolded state (Figure 3a). Expectedly, poly1 exhibits the desired NOE cross-peaks in the (E)-TMAB state, and no cross-peaks in the (Z)-TMAB state (Figure 3b). Due to the relatively low concentration of azobenzenes and cyclodextrins per polymer, many scans were required. To limit the amount of thermal relaxation back from (Z) to (E) azobenzene and to limit the amount of NMR instrument use time, free induction decay (FID) recordings were truncated to 20 ms because most of the analyte signal intensity is encoded in the first few FID points. This truncation resulted in crude NMR spectra with many truncation artifacts, but cross-peaks were nonetheless successfully be detected. Combined with the data obtained from the NOESY NMR data, the photoisomerization quantum yield data confirm inclusion between TMAB and βCD moieties within poly1, inducing self-folding behavior.

Determining poly1 acid-catalyzed irreversible unfolding behavior. The (Z)-to-(E) isomerization of azobenzenes has been demonstrated to be catalyzed by acids[44,45] and the protonated (E)-TMAB$^+$-H exhibits increased resonance stabilization due to intramolecular hydrogen bonding, rendering it unable to be isomerized back into its (Z) state.[43]

We determined the effect of deuterium chloride (DCl) on TMAB-TEG. DCl in D_2O was used to prevent a large water signal in the ^1H NMR spectra. First, ^1H NMR spectroscopy at 26.7 ºC was used to confirm that (1) H^+ catalyzes the relaxation of (Z)-TMAB from to (E)-TMAB and (2) H^+ stabilizes (E)-TMAB. For these experiments, TMAB-TEG was dissolved in an NMR tube and isomerized to (Z)-TMAB with green light. DCl in D_2O was injected into the NMR tube and immediately moved into the NMR spectrometer for data acquisition. Although TMAB-TEG showed negligible thermal relaxation in D_2O, it showed complete relaxation to (E)-TMAB within 30 minutes with the addition of DCl (Figure 1c). We then tried to photoisomerize the (E)-TMAB-TEG$^+$-H back to (Z)-TMAB. Irradiation with either 470 nm or 520 nm (UltraFire) light for up to 60 min showed no isomerization by ^1H NMR spectroscopy (data not shown), likely due to the stabilization of the planar 6-membered ring formed by the acidified TMAB-TEG. The same NOESY experimental conditions were used, and no cross-peaks were observed, indicating no folding behavior under acidic conditions (Figure 3c).

Conclusion. We demonstrate the reversible folding of a high molecular weight polymer in aqueous solution using only visible light. We also demonstrate the ability of our polymer system to respond to a second, non-thermal stimulus as it can undergo irreversible unfolding in response to acidic conditions. Folding behavior of poly1 was determined by a combination of illumination-dependent extinction spectroscopy and 2-D ^1H NOESY NMR experiments. These new light-responsive and pH-responsive polymers can be used for their ability to change their dimensions in response to external stimuli.

ASSOCIATED CONTENT

Supporting Information. Equipment details, chemical details, synthetic procedures, and custom NMR pulse programs, and additional figures and discussion are available in the Supporting Information. This material is available free of charge via the Internet at http://pubs.acs.org.

AUTHOR INFORMATION

Corresponding Author

* Email: spun@uw.edu

Author Contributions

The manuscript was written through contributions of all authors. All authors have given approval to the final version of the manuscript.

ACKNOWLEDGMENT

This work was supported by the University of Washington Office of Research. We acknowledge the support of the National Institute of Standards and Technology, U.S. Department of Commerce, in providing the neutron research facilities used in this work. Access to the NG-3 45 m very small-angle neutron scattering (SANS) instrument was provided by the Center for High Resolution Neutron Scattering, a partnership between the National Institute of Standards and Technology and the National Science Foundation under Agreement No. DMR-2010792. Support for SANS measurements presented in this work was provided by the Department of Energy Office of Basic Energy Sciences under awards DE-SC0019911 (LDP) and the EFRC Center for the Science of Synthesis Across Scales (CSSAS) DE-SC0019288 (KL).

ABBREVIATIONS

βCD, beta-cyclodextrin; DCl, deuterium chloride; DOSY, diffusion ordered spectroscopy; ECT, 4-Cyano-4-(ethylsulfanylthiocarbonyl) sulfanyl pentanoic acid; IPF, integrated photokinetic factor; GPC, gel permeation chromatography; NMR, nuclear magnetic resonance; NOE, nuclear Overhauser effect; NOESY, nuclear Overhauser effect spectroscopy; RAFT, reversible addition-fragmentation chain-transfer polymerization; TMAB, tetramethoxyazobenzene.

REFERENCES

[1] Z. Qian, D. S. Ginger, *J. Am. Chem. Soc.* **2017**, *139*, 5266–5276.

[2] S. Samai, Z. Qian, J. Ling, K. N. Guye, D. S. Ginger, *ACS Appl. Mater. Interfaces* **2018**, *10*, 8976–8984.

[3] T. Ding, V. K. Valev, A. R. Salmon, C. J. Forman, S. K. Smoukov, O. A. Scherman, D. Frenkel, J. J. Baumberg, *Proc. Natl. Acad. Sci. U. S. A.* **2016**, *113*, 5503–5507.

[4] S. Mura, J. Nicolas, P. Couvreur, *Nat. Mater.* **2013**, *12*, 991–1003.

[5] C. E. Wang, H. Wei, N. Tan, A. J. Boydston, S. H. Pun, *Biomacromolecules* **2016**, *17*, 69–75.

[6] P. Z. Elias, G. W. Liu, H. Wei, M. C. Jensen, P. J. Horner, S. H. Pun, *J. Control. Release* **2015**, *208*, 76–84.

[7] S. Wang, L. Yue, Z. Y. Li, J. Zhang, H. Tian, I. Willner, *Angew. Chemie - Int. Ed.* **2018**, *57*, 8105–8109.

[8] M. Yoon, J. E. Lee, Y. J. Jang, J. W. Lim, A. Rani, D. H. Kim, *ACS Appl. Mater. Interfaces* **2015**, *7*, 21073–21081.

[9] M. Wei, Y. Gao, X. Li, M. J. Serpe, *Polym. Chem.* **2017**, *8*, 127–143.

[10] B. Schuler, W. A. Eaton, *Curr. Opin. Struct. Biol.* **2008**, *18*, 16–26.

[11] J. I. L. Chen, Y. Chen, D. S. Ginger, *J. Am. Chem. Soc.* **2010**, *132*, 9600–9601.

[12] J. I. L. Chen, H. Durkee, B. Traxler, D. S. Ginger, *Small* **2011**, *7*, 1993–1997.

[13] M. Gränz, N. Erlenbach, P. Spindler, D. B. Gophane, L. S. Stelzl, S. T. Sigurdsson, T. F. Prisner, *Angew. Chemie - Int. Ed.* **2018**, *57*, 10540–10543.

[14] S. M. Kelly, C. Price, Nicholas, *Biochim. Biophys. Acta* **1997**, *1338*, 161–185.

[15] S. M. V. Freund, K. B. Wong, A. R. Fersht, *Proc. Natl. Acad. Sci. U. S. A.* **1996**, *93*, 10600–10603.

[16] B. V. K. J. Schmidt, N. Fechler, J. Falkenhagen, J. F. Lutz, *Nat. Chem.* **2011**, *3*, 234–238.

[17] J. P. Desvergne, H. Bouas-Laurent, *J. Chem. Soc. Chem. Commun.* **1978**, 403–404.

[18] O. Altintas, P. Gerstel, N. Dingenouts, C. Barner-Kowollik, *Chem. Commun.* **2010**, *46*, 6291–6293.

[19] N. Hosono, M. A. J. Gillissen, Y. Li, S. S. Sheiko, A. R. A. Palmans, E. W. Meijer, *J. Am. Chem. Soc.* **2013**, *135*, 501–510.

[20] J. Willenbacher, O. Altintas, P. W. Roesky, C. Barner-Kowollik, *Macromol. Rapid Commun.* **2014**, *35*, 45–51.

[21] G. Yilmaz, V. Uzunova, R. Napier, C. Remzi Becer, *Biomacromolecules* **2018**, *19*, 3040–3047.

[22] Y. Inoue, P. Kuad, Y. Okumura, Y. Takashima, H. Yamaguchi, A. Harada, *J. Am. Chem. Soc.* **2007**, *129*, 6396–6397.

[23] S. Jia, W.-K. Fong, B. Graham, B. J. Boyd, *Chem. Mater.* **2018**, *30*, 2873–2887.

[24] H. M. D. Bandara, S. C. Burdette, *Chem. Soc. Rev.* **2012**, *41*, 1809–1825.

[25] D. Wang, M. Wagner, H. J. Butt, S. Wu, *Soft Matter* **2015**, *11*, 7656–7662.

[26] E. Titov, L. Lysyakova, N. Lomadze, A. V. Kabashin, P. Saalfrank, S. Santer, *J. Phys. Chem. C* **2015**, *119*, 17369–17377.

[27] B. Xu, H. Qian, S. Lin, **2020**, DOI 10.1021/acsmacrolett.0c00079.

[28] L. Ding, H. Mao, J. Xu, J. He, X. Ding, T. P. Russell, D. R. Robello, M. Mis, *Macromolecules* **2008**, *41*, 1897–1900.

[29] S. P. Jeong, L. A. Renna, C. J. Boyle, H. S. Kwak, E. Harder, W. Damm, D. Venkataraman, *Sci. Rep.* **2017**, *7*, 1–12.

[30] X. Wang, Y. Yang, P. Gao, F. Yang, H. Shen, H. Guo, D. Wu, *ACS Macro Lett.* **2015**, *4*, 1321–1326.

[31] Y. C. Liu, A. L. M. L. Ny, J. Schmidt, Y. Talmon, B. F. Chmelka, C. T. Lee, *Langmuir* **2009**, *25*, 5713–5724.

[32] Y. Yan, S. Samai, K. L. Bischoff, J. Zhang, D. S. Ginger, *ACS Sensors* **2016**, *1*, 556–571.

[33] Y. Yan, J. I. L. Chen, D. S. Ginger, *Nano Lett.* **2012**, *12*, 2530–2536.

[34] Y.-L. Zhao, J. F. Stoddart, *Langmuir* **2009**, *25*, 8442–8446.

[35] S. Tamesue, Y. Takashima, H. Yamaguchi, S. Shinkai, A. Harada, *Angew. Chemie - Int. Ed.* **2010**, *49*, 7461–7464.

[36] I. Tomatsu, A. Hashidzume, A. Harada, *Macromolecules* **2005**, *38*, 5223–5227.

[37] D. Tarn, D. P. Ferris, J. C. Barnes, M. W. Ambrogio, J. F. Stoddart, J. I. Zink, *Nanoscale* **2014**, *6*, 3335.

[38] D. P. Ferris, Y.-L. Zhao, N. M. Khashab, H. A. Khatib, J. F. Stoddart, J. I. Zink, *J. Am. Chem. Soc.* **2009**, *131*, 1686–1688.

[39] Q. Bian, S. Chen, Y. Xing, D. Yuan, L. Lv, G. Wang, *Acta Biomater.* **2018**, *76*, 39–45.

[40] S. Ito, H. Akiyama, M. Mori, M. Yoshida, H. Kihara, *Macromol. Chem. Phys.* **2019**, *1900105*, 1900105.

[41] Y. Wang, N. Ma, Z. Wang, X. Zhang, *Angew. Chemie - Int. Ed.* **2007**, *46*, 2823–2826.

[42] H. Asanuma, X. Liang, H. Nishioka, D. Matsunaga, M. Liu, M. Komiyama, *Nat. Protoc.* **2007**, *2*, 203–212.

[43] S. Samanta, A. Babalhavaeji, M. X. Dong, G. A. Woolley, *Angew. Chemie - Int. Ed.* **2013**, *52*, 14127–14130.

[44] A. M. Sanchez, M. Barra, R. H. De Rossi, *J. Org. Chem.* **1999**, *64*, 1604–1609.

[45] M. Azuki, K. Morihashi, T. Watanabe, O. Takahashi, O. Kikuchi, *J. Mol. Struct. THEOCHEM* **2001**, *542*, 255–262.

[46] A. A. Beharry, O. Sadovski, G. A. Woolley, *J. Am. Chem. Soc.* **2011**, *133*, 19684–19687.

[47] S. Wu, L. Niu, J. Shen, Q. Zhang, C. Bubeck, *Macromolecules* **2009**, *42*, 362–367.

[48] P. Weis, D. Wang, S. Wu, *Macromolecules* **2016**, *49*, 6368–6373.

[49] E. R. Talaty, J. C. Fargo, *Chem. Commun.* **1967**, 65–66.

[50] H. Rau, E. Lüddecke, *J. Am. Chem. Soc.* **1982**, *104*, 1616–1620.

[51] T. Ikegami, N. Kurita, H. Sekino, Y. Ishikawa, *J. Phys. Chem. A* **2003**, *107*, 4555–4562.

[52] S. Samai, D. J. Bradley, T. L. Y. Choi, Y. Yan, D. S. Ginger, *J. Phys. Chem. C* **2017**, *121*, 6997–7004.

[53] Y. Yan, X. Wang, J. I. L. Chen, D. S. Ginger, *J. Am. Chem. Soc.* **2013**, *135*, 8382–8387.

[54] P. Bortolus, S. Monti, *J. Phys. Chem.* **1987**, *91*, 5046–5050.

[55] J. Royes, C. Courtine, C. Lorenzo, N. Lauth-De Viguerie, A. F. Mingotaud, V. Pimienta, *J. Org. Chem.* **2020**, *85*, 6509–6518.

[56] E. Sabadini, T. Cosgrove, F. do C. Egídio, *Carbohydr. Res.* **2006**, *341*, 270–274.

[57] H.-J. Schneider, F. Hacket, V. Rüdiger, H. Ikeda, *Chem. Rev.* **1998**, *98*, 1755–1785.

SYNOPSIS TOC (Word Style "SN_Synopsis_TOC"). If you are submitting your paper to a journal that requires a synopsis graphic and/or synopsis paragraph, see the Instructions for Authors on the journal's homepage for a description of what needs to be provided and for the size requirements of the artwork.

To format double-column figures, schemes, charts, and tables, use the following instructions:

Place the insertion point where you want to change the number of columns
From the **Insert** menu, choose **Break**
Under **Sections**, choose **Continuous**
Make sure the insertion point is in the new section. From the **Format** menu, choose **Columns**
In the **Number of Columns** box, type **1**
Choose the **OK** button

Now your page is set up so that figures, schemes, charts, and tables can span two columns. These must appear at the top of the page. Be sure to add another section break after the table and change it back to two columns with a spacing of 0.33 in.

Table 1. Example of a Double-Column Table

Column 1	Column 2	Column 3	Column 4	Column 5	Column 6	Column 7	Column 8

Authors are required to submit a graphic entry for the Table of Contents (TOC) that, in conjunction with the manuscript title, should give the reader a representative idea of one of the following: A key structure, reaction, equation, concept, or theorem, etc., that is discussed in the manuscript. Consult the journal's Instructions for Authors for TOC graphic specifications.

Insert Table of Contents artwork here